Positron trapping rates and their temperature dependencies in electron-irradiated silicon

P. Mascher,* S. Dannefaer, and D. Kerr
Department of Physics, University of Winnipeg, Winnipeg, Manitoba, Canada R3B 2E9
(Received 5 June 1989)

Defects created by 2-MeV electron irradiation of Czochralski-grown silicon have been investigated with use of positron-lifetime spectroscopy and results have been correlated with EPR and ir data. The trapping rate for the positrons was smallest for the neutral divacancy where a concentration of $\sim 10^{17}$ cm^{-3} gave rise to a trapping rate of 1 ns^{-1}. For the singly negative divacancy the trapping rate was increased at 300 K by a factor of about 3.5 and for the doubly negative divacancy a further increase by a factor of 2 was found. Isochronal annealing showed that the neutral divacancy annealed at only 150 °C, while the charged states annealed in a broad temperature range starting at 230 °C. The monovacancy component found in some of the samples could be identified as being due to divacancy-oxygen complexes. Measurements in thermal equilibrium between 30 K and room temperature showed that shallow positron traps became activated at low temperatures. Oxygen vacancy pairs (A centers) are concluded to be the defects acting as shallow traps and yielded a lifetime of 225 ps, very close to the bulk lifetime of silicon. The trapping cross section of the charged defects varied with temperature as T^{-n}, with $2 < n < 3$.

I. INTRODUCTION

In recent years it has been shown that positron-annihilation spectroscopy (PAS) can contribute significantly to the understanding of fundamental defect properties in semiconductors in general and in silicon in particular.[1–3] However, the long-standing problem of associating a certain positron response with the concentration of defects causing this response has so far impeded the use of PAS as compared to established techniques such as electron paramagnetic resonance (EPR), deep-level transient spectroscopy (DLTS), or infrared (ir) spectroscopy. The aim of the investigations reported in this paper was to solve this problem by using EPR data on electron-irradiated silicon[4,5] as a gauge for the PAS results. We will show that both a clear identification of defects created by electron irradiation in silicon and a quantitative link between defect concentration and positron trapping rate can be established.

Irradiation of Czochralski-grown silicon (Cz-Si) with 2-MeV electrons at room temperature creates both monovacancies and divacancies as primary defects.[6–9] However, since only the monovacancies are mobile at room temperature, the resulting defect pattern will consist of divacancies and monovacancies trapped by the interstitital oxygen.[8] Because of the much higher introduction rate of monovacancies compared to that of divacancies, the dominant defect will be the oxygen-vacancy pair with an effective introduction rate that depends on the concentration of interstitial oxygen. The introduction rates of the other important defects are about 0.01 cm^{-1} for the divacancies[6] and about 50% of the A-center introduction rate for V_2O complexes.[10] Dopants (such as phosphorus) usually compete in the trapping of vacancies with the oxygen and form their own complexes.[11]

The selection of samples ranging from heavily n type to slightly p type also made it possible to investigate the effects of various charge states of particular defects on the trapping of positrons and their dependence on temperature.

II. EXPERIMENTAL DETAILS

Samples of Cz-Si were investigated by positron-lifetime spectroscopy after irradiation with 2-MeV electrons at room temperature to a dose of 1×10^{18} e^-/cm^2. Both the electron energy and the irradiation dose used in our experiments were very similar to the parameters in the EPR investigations mentioned in the Introduction to facilitate quantitative comparisons. The samples were isochronally annealed in air up to about 400 °C ($t_A = 30$ min) and quenched within a few seconds to room temperature where the lifetime spectra were taken. Some of the samples were also investigated in thermal equilibrium between room temperature and 30 K, both "as-irradiated" and after the highest annealing temperature.

The positron-lifetime spectra were obtained using two spectrometers having time resolutions of 240 and 255 ps (full width at half maximum), respectively, and different efficiencies. The less efficient spectrometer was used for the room-temperature measurements where directly deposited positron sources (3–3.5 μCi) were used in close geometry. No measurable source component could be identified. The more efficient spectrometer was used for the low-temperature measurements to compensate for the wider detector separation due to the cryostat. There, a foil-source arrangement consisting of 8.2-μCi ^{22}NaCl enclosed by a 1-mg/cm^2 Al foil was used. The now-necessary source correction consisted of a 251-ps component with 1.6% intensity (due to the annihilation in the

 ©1989 The American Physical Society

Al foil). We also expected to obtain a contribution from annihilations in the NaCl itself (with a lifetime of about 450 ps), but comparisons with spectra taken with the weak directly deposited sources did not reveal any discernible differences.

The lifetime spectra, containing at least 6.5×10^6 counts per spectrum, were analyzed by POSITRONFIT (Ref. 12) and were typically decomposed into three components, the longest of which, however, was an essentially constant term of about 1.5 ns with no more than 0.3% intensity. This term could easily be separated from the actual spectra, leaving two significant terms from the silicon itself. In some cases a third significant term was necessary to properly describe the spectrum.

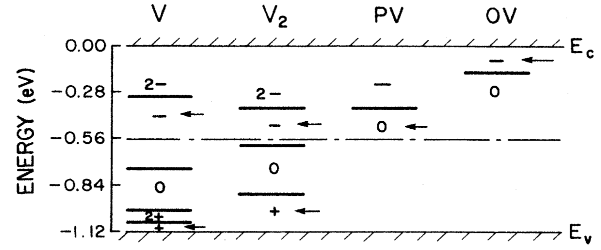

FIG. 1. Energy levels for various charge states of mono- and divacancies, PV pairs (E center), and OV pairs (A center) in Si (Ref. 15). EPR-active (spin-$\frac{1}{2}$) states are indicated by arrows. V_2O (not shown) has no reported levels in the band gap and is a spin-1 center.

III. RESULTS

The samples listed in Table I are characterized by different concentration levels of interstitial oxygen, O_I, giving rise to different concentrations of oxygen-vacancy pairs after irradiation as determined by infrared absorption.[13] For the upcoming discussion of the experiment, the samples are grouped according to their Fermi-level positions[14] as indicated in Table I after irradiation. Figure 1 shows the energy levels for various charge states of the main defects in Cz-Si introduced by electron irradiation.[15] The divacancy-oxygen center (not shown) has no reported levels in the band gap.

A. Isochronal annealing

The results in this section are presented according to the three groups of samples in Table I beginning with the slightly n-type samples 2, 3, and 4 which showed the least complex behavior. Both samples 2 and 3 showed only two significant lifetimes (see Table II), the longer of which, $\tau_2 \approx 320$ ps, can be identified as the lifetime of positrons trapped in divacancies.[16,17] The shorter component, $\tau_1 \equiv 1/\lambda_1$, represents the lifetime in the bulk, $\tau_B \equiv 1/\lambda_B$, modified by the trapping process according to the two-state trapping model:[18]

$$\tau_1=(\lambda_B+\kappa)^{-1} , \quad (1)$$

with the trapping rate, κ, given by

$$\kappa=(\lambda_B-\lambda_2)[I_2/(1-I_2)] , \quad (2)$$

where $\lambda_2 \equiv 1/\tau_2$ is the annihilation rate in the trap and I_2 the intensity of this component directly determined by the fitting procedure.

The applicability of the trapping model can be verified in the following way. Using Eqs. (1) and (2) the bulk lifetime can be calculated using the experimentally obtained values for τ_1 and τ_2 and their corresponding intensities:

$$\tau_B=(I_1/\tau_1+I_2/\tau_2)^{-1} . \quad (3)$$

Since τ_B is a material constant (which for silicon has the value of 218 ps essentially independent of sample temperature[3]) the calculated values should be close to this value if the trapping model is indeed applicable. This verification is important since the physically important trapping rate is based on the trapping model.

In Fig. 2 are shown the trapping rates into divacancies as a function of isochronal annealing in samples 2, 3, and 4. Together with the trapping rates is shown the annealing behavior of (negatively charged) divacancies as determined by EPR experiments.[4] In the case of sample 4, τ_2 (311±3 ps) was slightly shorter but it was possible to split this component into $\tau_2=270$ and $\tau_3=320$ ps, where

TABLE I. Characteristics of the investigated Cz-Si samples.

Sample no.	Doping characteristics (before irradiation)	$[O_I]$ (10^{17} cm^{-3})	$[OV]$ (10^{17} cm^{-3}) (after irradiation)	Fermi level E_F (eV) (after irradiation)
1	n type, P doped, $\rho\approx0.1$ Ω cm	4.3	≈1.0	$E_F \simeq E_c-0.17$
2	n type, $\rho=5-10$ Ω cm	1.9	0.15	$E_c-0.56<E_F<E_c-0.41$
3		2.6	0.28	
4		2.7	0.53	
5	p type, $\rho=5-10$ Ω cm	5.9	0.79	$E_F<E_c-0.60$
6		6.0	0.86	
7		6.7	1.10	

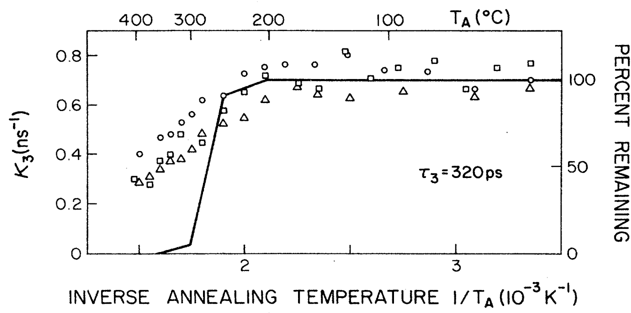

FIG. 2. Trapping rates κ_3 as a function of isochronal annealing of the slightly n-type samples 2 (○), 3 (△), and 4 (□). Also shown by the solid line is the annealing of (negatively charged) divacancies from EPR data (Ref. 4).

270 ps is the well-established lifetime value for positrons trapped in monovacancy-type defects.[3] The trapping rate for this component was constant at 0.20±0.06 ns^{-1}.

Figure 3 shows the lifetime results as a function of isochronal annealing of sample 1 (highly P doped). In this case it was necessary to separate three significant components (see Table II), representing divacancies (τ_3=325 ps), a monovacancy-type defect (τ_2=270 ps), and the modified bulk lifetime. As a consequence, the two-state-trapping model has to be expanded to accommodate a second defect-related component. The new expressions for the trapping rates then are

$$\kappa_2=[\lambda_B-\lambda_2(1-I_3)-I_3\lambda_3](I_2/I_1) \quad (4)$$

and

$$\kappa_3=[\lambda_B-\lambda_3(1-I_2)-I_2\lambda_2](I_3/I_1) \quad (5)$$

with $\lambda_i \equiv 1/\tau_i$ and $\sum_i I_i=1$. The lifetime in the bulk, τ_B, then becomes

$$\tau_B=(I_1/\tau_1+I_2/\tau_2+I_3/\tau_3)^{-1} \, . \quad (6)$$

From Fig. 3 one can see that only for $T_A > 156\,°C$ is the trapping model satisfied with τ_B=218 ps. This means that for $T_A < 156\,°C$ the trapping rates κ_2 and κ_3 cannot be calculated properly using Eqs. (4) and (5), and hence,

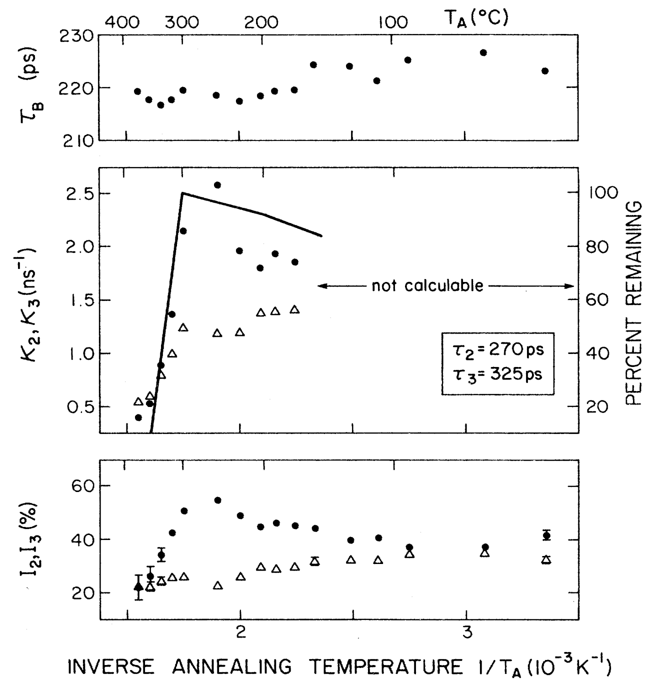

FIG. 3 Trapping rates κ_2 (●) and κ_3 (△) as a function of isochronal annealing of sample 1 (P-doped, n type). Also shown by the solid line is the annealing of V_2O complexes from EPR data (Ref. 5).

they are not included in Fig. 3. The annealing behavior shown for V_2O complexes was taken from EPR experiments.[5]

In Fig. 4 the trapping rates in sample 7—representative of the p-type materials—are shown as a function of isochronal annealing. Because of the low trapping rates, it is difficult to reliably separate more than two lifetime components. Since only one defect-related component with τ_2=270±3 ps could be found above T_A=130 °C, this component was fixed for $T_A < 130\,°C$ as well, leading to τ_3 values in the range from 320 to 325 ps and the trapping rates κ_2 and κ_3 shown in the figure.

TABLE II. Original decomposition of the lifetime spectra at room temperature. Results of three- and four-term fits are shown in the upper and lower parts of the table, respectively. A spurious long-lived component present in all spectra is not shown. (F) denotes lifetime component fixed in the analysis.

Parameter	Sample no. 1	2	3	4	7
τ_1 (ps)	statistically	188±2	192±2	181±2	195±2
τ_2 (ps)	not	318±3	321±3	311±3	300±5
I_2 (%)	acceptable	35±2	31±2	43±2	30±3
τ_1 (ps)	133±6	no further		180±2	192±3
τ_2 (ps)	270±14	decomposition		270 (F)	270 (F)
τ_3 (ps)	325 (F)	possible		320 (F)	320–325 (F)
I_2 (%)	42±5			15±4	23–26 (±5)
I_3 (%)	32±6			31±2	13–11 (±2)

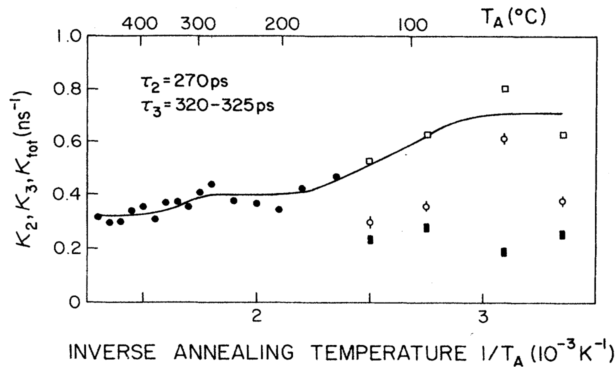

FIG. 4. Trapping rates κ_2 (○,●), κ_3 (■), and total trapping rate κ_{tot} (□) as a function of isochronal annealing of sample 7 (p type). The solid line is to guide the eye only.

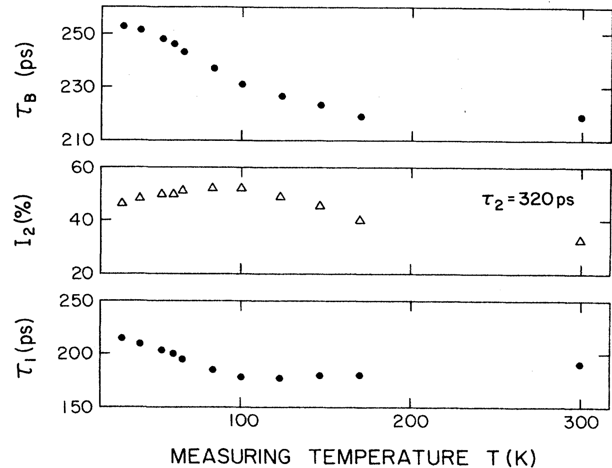

FIG. 6. Lifetime component τ_1, intensity of the second lifetime component (τ_2=320 ps), I_2, and bulk lifetime τ_B, as calculated from Eq. (3) as a function of measuring temperature in sample 2 (slightly n type).

B. Measurements in thermal equilibrium

Samples 1, 2, and 7 were also investigated in thermal equilibrium between room temperature and 30 K, both "as-irradiated" and after quenching from the highest annealing temperature.

Figure 5 shows the results for sample 1 in the as-irradiated state. Between room temperature and 135 K, both τ_1 and τ_2 increase with decreasing temperature, albeit τ_2 much less rapidly than τ_1. Below 135 K, τ_1 and τ_2 are constant at 225 and 325 ps, respectively, while I_2 still shows a pronounced temperature dependence. Importantly, the calculated bulk lifetimes now show very large deviations from 218 ps. The figure shows only the results of a two-term fit since the splitting (above T=135 K) of τ_2 into a 270- and a 325-ps component has very little influence on the first (shortest) component and does not alter the calculated τ_B values at all. The observed temperature dependence and the strong variations of τ_B—as calculated from the simple trapping model—show that this model cannot satisfactorily describe these data. Sample 2 (slightly n type) shows, in general, the same temperature effect—see Fig. 6—with the onset of the increase in τ_1 shifted down to about 100 K. In this sample τ_2=320 ps is constant and hence is the true representation of the lifetime in divacancies. Since these two samples clearly exhibit spectra which are not understandable in terms of the simple trapping model, a modified version and its consequences will be discussed in the next section.

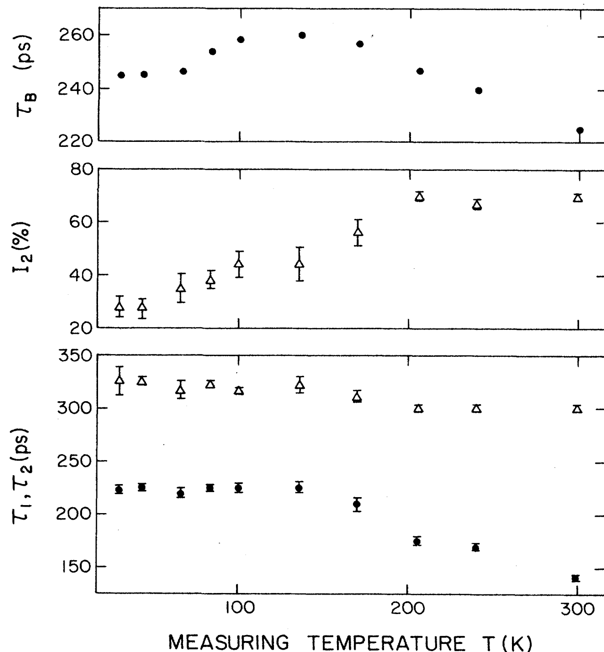

FIG. 5. Lifetime components τ_1 (●) and τ_2 (△), intensity of the second component, I_2, and bulk lifetime τ_B, as calculated from Eq. (3) as a function of measuring temperature in sample 1 (P doped, n type).

Contrasting these strong temperature dependencies for the as-irradiated state the same samples annealed at 400 °C showed a much reduced temperature dependence of the lifetimes and intensities between room temperature and 30 K. The lightly doped sample showed no temperature effect, while the phosphorus-doped sample retained some of the temperature effect in that τ_B increased to a level of 232 ps around 100 K, considerably less than the 260 ps in the as-irradiated state. No temperature dependence of the lifetime parameters could be found for the p-type sample.

IV. DISCUSSION

This section is subdivided into two parts. In Sec. IV A the annealing data will be discussed with respect to defect identification and quantification, and Sec. IV B will deal with the temperature dependencies.

A. Positron trapping at room temperature

The main difference between our samples is due to doping (both type and dopant concentration) and, as a consequence, the charge states of the observed defects. According to Watkins and Corbett[4] (Fig. 1) the divacancies in sample 1 should be in the doubly negative charge state,[14,19] in sample 2 (predominantly) in the singly negative charge state, and in sample 7 (predominantly) in the neutral state.[14,20]

The comparison of the annealing behavior of the 320-ps component with the annealing of (negatively charged) divacancies as found by EPR experiments (Fig. 2) clearly substantiates the identification of this component as being due to trapping in divacancies. The fact that above 250 °C the annealing of the trapping rate is less steep than the EPR curve is an indication for the formation of other complexes with divacancy character (such as V_3O). The positrons would still "see" them essentially as divacancies whereas the EPR signal is strictly associated with free divacancies, and indeed the generation through annealing of more and more complex defects in the presence of oxygen is well established.[15,10] Having thus established, by comparison with EPR data, that the 320–325-ps lifetime is indeed due to divacancies, we now proceed to discuss trapping rates as well as their dependence on charge states.

The trapping rate, κ, may be written

$$\kappa = \nu_D C_D \ , \quad (7)$$

where ν_D is the specific trapping rate of defect D and C_D is the concentration of this defect. Since we are dealing with trapping of positively charged particles, the specific trapping rate will substantially increase when defects become negatively charged.

Divacancies are produced by 2-MeV electron irradiation as primary defects[6,7] at a rate of about 0.01 cm^{-1} at room temperature.[6] We should therefore expect in our samples a concentration of divacancies, $[V_2]$, of about 1×10^{16} cm^{-3}. Since the trapping rate, κ_3, into the neutral divacancy, $V_2{}^0$, in the p-type sample (Fig. 4) is 0.2 ns^{-1}, the specific trapping rate is 2×10^{-17} $ns^{-1}\,cm^3$ (or 1×10^{15} s^{-1} per unit divacancy concentration). This value is actually an upper limit for the specific trapping rate since the low dopant concentration in sample 7 could result in a contribution from negatively charged divacancies (see Table I and Fig. 1). Figures 2 and 3 show that the trapping rates into divacancies in the slightly and strongly n-type samples are about 0.7 and 1.4 ns^{-1}, respectively. By comparison with Table I and Fig. 1, we thus conclude that the transition from the neutral to the singly negative charge state yields about a factor 3.5 increase in the specific trapping rate and the transition to doubly negatively charged divacancies yields another factor 2.

Further support for these quantitative links can be obtained by means of the V_2O defect. It is produced at about half the rate of the [OV] center[10] and is neutral, at least in samples 2–7. This leads to expected V_2O concentrations, $[V_2O]$, of about 0.26×10^{17} and 0.55×10^{17} cm^{-3} in samples 4 and 7, respectively (see Table I). The experimentally determined trapping rates are $\kappa_2 \simeq 0.2$ ns^{-1} in sample 4 (Sec. III A) and $0.4 < \kappa_2 < 0.6$ ns^{-1} in sample 7 (Fig. 4). Both samples thus yield a specific trapping rate $\nu_D = 1\times10^{-17}$ $ns^{-1}\,cm^3$. The neutral V_2O defect hence exhibits nearly the same specific trapping rate as the neutral divacancy which is only to be expected. These rates are essentially the same as the value found recently for neutral defects in GaAs (Ref. 21) and are also in agreement with trapping rates usually found in metals.[22]

It is noteworthy that in sample 1 the trapping rate into monovacancy-type defects is substantially higher than that due to the V_2O concentration alone, which by itself should contribute only with ~ 0.5 ns^{-1}. The additional monovacancy contribution is undoubtedly due to the fairly high phosphorus concentration in this sample, which leads to the formation of phosphorus-vacancy pairs (E centers).[11,13]

Figure 4 shows that trapping into neutral divacancies could not be observed for annealing temperatures $T_A \geq 130$ °C. This leads us to the conclusion tat the neutral divacancy exhibits a distinctly different annealing behavior than the charged species. At the present time it is not known whether the neutral divacancies are annihilated by interstitials[23] (or interstitial impurity complexes[24]) or have a significantly lower migration energy than the charged ones. Another possibility is that the divacancies do not actually anneal at these low temperatures, but are rendered invisible to the positrons by a shift in the Fermi-level position. This idea is supported by recent results obtained by Svensson *et al.*,[25] who observed in highly boron-doped samples a strong dependence of the ir-absorption bands on the Fermi-level position during annealing *below* 200 °C. They attributed this to a change of the divacancy charge state from neutral to singly positive. Further experiments on p-type materials—preferably with higher defect concentrations to obtain a stronger positron response—are necessary to solve this interesting problem.

At this point it is worth noting that, from the annealing experiments, there is no *direct* evidence for positrons being trapped by A centers despite their large abundance compared to all other defects. From Fig. 1 and the Fermi-level ranges in Table I one can see that the A centers are neutral in samples 2–7, while in sample 1 both the neutral and the singly negative charge state are occupied with about equal concentrations.[19] One should, therefore, expect to obtain the strongest response from trapping by A centers—if any—in sample 1. Figure 3 shows that up to annealing temperatures $T_A \sim 150$ °C the bulk lifetime calculated from Eq. (6) is consistently high by about 5 ps compared to the expected value of $\tau_B = 218$ ps obtained for all the other samples. In the following section on the temperature dependencies of positron trapping it will be shown that this apparent "increase" in τ_B is due to A centers acting as shallow positron traps.

B. Temperature dependencies

Figure 5 shows the lifetime data as a function of temperature for sample 1 (highly P doped) in the as-irradiated state. The pronounced temperature depen-

dence of the bulk lifetime, τ_B, as calculated from Eq. (6) shows that the simple trapping model is not sufficient to explain the experimental results.

From the figure, one can see that in sample 1 for temperatures lower than 135 K a constant lifetime component with $\tau=225$ ps emerges in addition to the divacancy component. The value of 225 ps is slightly higher than that of the bulk lifetime. Therefore, it certainly cannot be due to a bulk component modified by trapping into the divacancies since this would require the lifetime to be shorter than 218 ps [cf. Eq. (1)]. The closeness of the lifetime value to that of the bulk lifetime indicates very little—if any—vacancy character of the responsible defect. Since in the oxygen-vacancy pair the oxygen occupies an almost substitutional position,[8] this, and the fact that the *A* centers are, in terms of their concentration, the dominant defects in our samples, lead us to the identification of the traps as *A* centers. Figure 5 shows a strongly temperature-dependent contribution of the *A* centers to the overall trapping picture which will be described in detail using the extended trapping model developed below.

The expansion of the simple trapping model to provide a more satisfactory description of the measured data involves the concept of shallow positron traps[26] and by implication detrapping out of these traps. One assumes that positrons at time $t=0$ occupy *only* the bulk state and that the shallow state is fed with a trapping rate, κ_{12}, and is also depopulated with a detrapping rate, δ_{21}. Trapping into one of the deep states only takes place via the bulk state with the rate κ_{13} and no detrapping is assumed to take place from a deep state. At low temperatures, where $\delta_{21}=0$, up to three lifetimes (depending on the amount of trapping) could therefore emerge experimentally: the modified bulk lifetime τ_1 $(1/\tau_1=1/\tau_B+\kappa_{12}+\kappa_{13})$, the shallow-state lifetime τ_2, and the lifetime in the deep trap, τ_3. In our case, however, due to the closeness of τ_1 and the lifetime in the shallow traps (which is very similar to the bulk lifetime) a separation of these two components is not experimentally possible. Using the formalism developed by Pagh *et al.*,[27] we obtain an expression for the detrapping rate:

$$\delta_{21}=\{1-[\alpha(1-I_3)/I_3-(\lambda_B-\lambda_3)/\kappa_{12}]^{-1}\}(\lambda_3-\lambda_2) , \quad (8)$$

where $\alpha=\kappa_{13}/\kappa_{12}$. A second relation between trapping and detrapping is given by

$$\lambda_2\kappa_{12}+(\lambda_2+\delta_{21}-\lambda_-)\left[\lambda_B+\frac{\lambda_3\kappa_{13}}{\lambda_3-\lambda_-}\right] =\lambda_+\lambda_-^2(1-I_3)(\tau_{e1}-1/\lambda_+) \quad (9)$$

with $\lambda_\pm=\frac{1}{2}(a+b\pm d)$ and

$$a=\lambda_B+\kappa_{12}+\kappa_{13} ,$$

$$b=\lambda_2+\delta_{21} ,$$

$$d=[(a-b)^2+4\kappa_{12}\delta_{21}]^{1/2} ,$$

where λ_B, λ_2, and λ_3 are the annihilation rates from the bulk state, the shallow trap, and the deep trap, respectively. τ_{e1} is the experimentally observed shortest lifetime component. I_3 is the intensity of the λ_3 component. Equations (8) and (9) involve three unknowns: δ_{21}, κ_{12}, and κ_{13}. Making use of the physical constraint that all the rates must be greater than or at least equal to zero, an iterative procedure leads to the allowed ranges for κ_{12} and κ_{13} shown in Fig. 7. This procedure also leads to a finite range $0\le\delta_{21}\le\delta_{max}$; only the maximum detrapping rates, δ_{max}, are shown in the figure. The trapping rates increase rapidly with decreasing temperature and below 135 K attain such large values that essentially all positrons are trapped.

Similar calculations were done for the slightly *n*-type material (sample 2), see Fig. 8. In this sample the *A* centers are neutral at room temperature and no contribution to the overall trapping could be found down to about 140 K, below which, however, a strong increase in the trapping rate into the *A* centers takes place. This indicates that more and more *A* centers become negatively charged, exhibiting the usual significant temperature dependence of the trapping cross section. The trapping rate into divacancies, κ_{13} increases of course also with decreasing temperature since most of the divacancies are

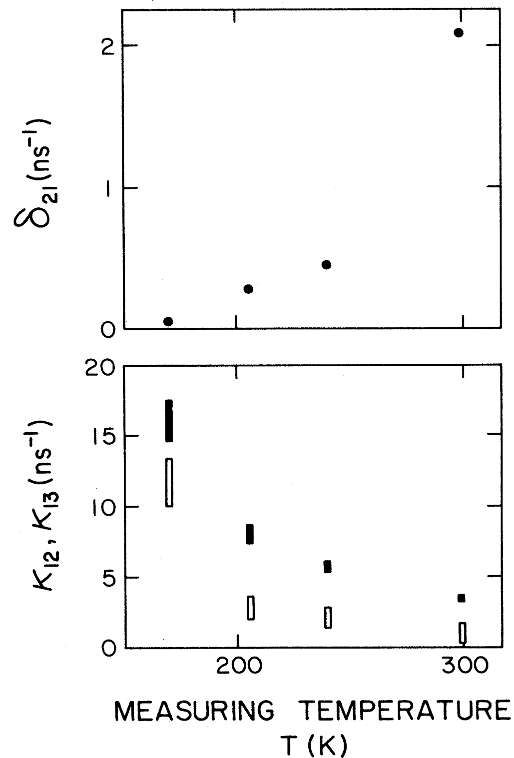

FIG. 7. Trapping rates into vacancy-type defects, κ_{13} (■), and into shallow traps, κ_{12} (□), as a function of measuring temperature in sample 1 (P doped, *n* type). Also shown are the maximum values of the detrapping rates δ_{21} out of the shallow traps.

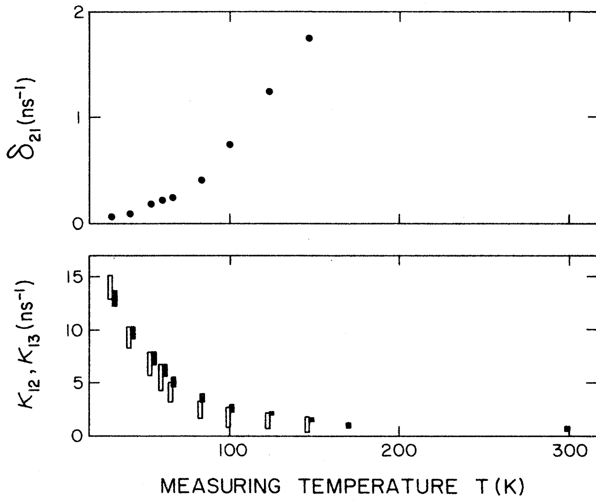

FIG. 8. Trapping rates into divacancies, κ_{13} (■), and into shallow traps, κ_{12} (□), as a function of measuring temperature in sample 2 (slightly n type). Also shown are the maximum values of the detrapping rates, δ_{21}, out of the shallow traps.

negatively charged already at room temperature.

In order to quantify the strong temperature dependence of the trapping rates, we will make use of Lax's[28] calculations regarding the trapping of electrons or holes by charged defects. The concept is that of cascade capture, meaning a process where a particle is first captured in a highly excited state of binding energy $\approx kT$. It, then, by emission of phonons, is progressively de-excited until it reaches a low energy level, eventually the ground state. If only acoustic phonons are important in the trapping process, the trapping cross section varies as $T^{-1.5}$, whereas optical phonons yield a T^{-n} dependence with n

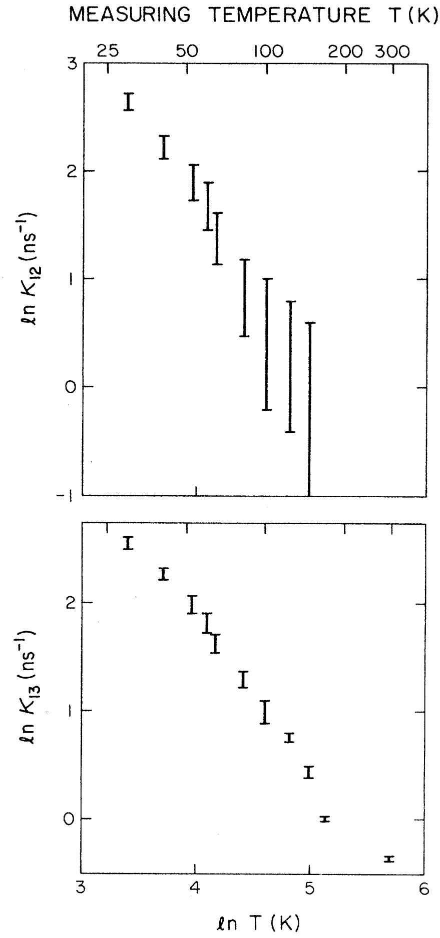

FIG. 9. Temperature dependence of the trapping rates κ_{12} and κ_{13} in sample 2 (slightly n type). The underlying model is described in the text.

TABLE III. Positron lifetimes in electron-irradiated Cz-Si at room temperature.

Sample no.	Characteristic lifetimes (ps)	Defects and their charge states	Specific trapping rate, ν_D, relative to $\nu_D^0=(1-2)\times10^{-17}$ cm^3/ns	Temperature dependence
1	$(\tau_{ST}=225)$[a]	O·V neutral and singly negative	not calculable	strong[b]
	$\tau_V=270$	V_2O neutral	not calculable	
		P·V singly negative		
	$\tau_{2V}=325$	V_2 doubly negative	7	
2,3	$\tau_{2V}=320$	V_2 singly negative	3.5	$T^{-(2-3)}$
4	$\tau_V=270$	V_2O neutral	1	none
	$\tau_{2V}=320$	V_2 singly negative	3.5	$T^{-(2-3)}$
5–7	$\tau_V=270$	V_2O neutral	1	none
	$\tau_{2V}=320-325$	V_2 neutral	1	none

[a]Observable below 150 K.
[b]Complete trapping makes T^{-n} fit impossible.

varying from 1 (at low temperatures) to 4 (at high temperatures). For neutral defects, essentially no temperature dependence of the trapping cross section is predicted. Considering now the temperature dependence of the trapping of positrons, we can write Eq. (7) as

$$\kappa=(2kT/m_+)^{1/2}\sigma_D(T)C_D \ , \qquad (10)$$

where the defect concentration, C_D, is assumed to be temperature independent. Following the arguments above we assume the specific trapping cross section σ_D, to be temperature dependent as T^{-n} so that a plot of $\ln\kappa$ versus $\ln T$ then will yield the value of n via the slope of the curve. Figure 9 shows such plots for κ_{12} and κ_{13} (the trapping rates into shallow traps and divacancies, respectively) in sample 2. The obtained n values lie between 2 and 3, which is in excellent agreement with $n=3.1$ found recently for low-temperature electron-irradiated float-zone silicon[29] and with the average n value of 2.5 found much earlier for neutron-irradiated silicon.[16] Unfortunately, for the P doped sample the small temperature range before reaching complete trapping makes a reliable determination of the n value impossible.

The absence of strong temperature dependencies after annealing at 400 °C is likely a result of complex formation of the residual defects.[5,10,30] These complexes are neutral and are typically oxygen-vacancy agglomerates. Depending on the particular makeup of individual complexes they may exhibit vacancy character (Figs. 2 and 4) or they may act as shallow traps, comparable to the A centers.

V. CONCLUSIONS

The reported results obtained by positron-lifetime spectroscopy on electron-irradiated Cz-Si are shown in Table III and can be summarized as follows. The investigation of isochronal annealing makes it possible—through correlation with EPR data—to associate lifetimes of 320–325 and 270 ps with trapping in divacancies and oxygen-divacancy complexes, respectively. The trapping rates for the neutral species at room temperature are very similar having values of 1–2 ns^{-1} for a defect concentration of 10^{17} cm^{-3}. If the defects are charged, the specific trapping rates (at room temperature) are increased by factors of 3.5 and 7 for singly and doubly negative charge states, respectively. In this case the specific trapping cross section is dependent on temperature as T^{-n} with $2<n<4$. Oxygen-vacancy pairs act as shallow traps with lifetimes close to the bulk value. In the negative charge state they exhibit essentially the same temperature dependence of the trapping cross section as do the charged divacancies.

ACKNOWLEDGMENTS

We would like to thank Dr. Lennart Lindström, Försvarets Forskningsanstalt (Linköping, Sweden), for the samples and their characterization. This work has been supported by the Natural Sciences and Engineering Research Council of Canada.

*Present address: Department of Engineering Physics, McMaster University, Hamilton, Ontario, Canada L8S 4M1.

[1] S. Dannefaer, P. Mascher, and D. Kerr, Phys. Rev. Lett. **56**, 2195 (1986).
[2] S. Dannefaer, Phys. Status Solidi A **102**, 481 (1987).
[3] S. Dannefaer, in *Defects in Semiconductors,* Vols. 10–12 of *Materials Science Forum,* edited by H. J. von Bardeleben (Trans Tech, Aedermannsdorf, Switz., 1986), p. 103.
[4] G. D. Watkins and J. W. Corbett, Phys. Rev. **138**, A543 (1965).
[5] Y. H. Lee and J. W. Corbett, Phys. Rev. B **13**, 2653 (1976).
[6] J. W. Corbett and G. D. Watkins, Phys. Rev. **138**, A555 (1965).
[7] O. O. Awadelkarim, Physica B **150**, 312 (1988).
[8] G. D. Watkins and J. W. Corbett, Phys. Rev. **121**, 1001 (1961).
[9] J. W. Corbett, G. D. Watkins, R. M. Chrenko, and R. S. McDonald, Phys. Rev. **121**, 1015 (1961).
[10] J. W. Corbett, G. D. Watkins, and R. S. McDonald, Phys. Rev. **135**, A1381 (1964).
[11] G. D. Watkins and J. W. Corbett, Phys. Rev. **134**, A1359 (1964).
[12] P. Kirkegaard and M. Eldrup, Comput. Phys. Commun. **7**, 410 (1974).
[13] J. L. Lindström (private communication).
[14] J. Svensson, B. G. Svensson, and B. Monemar, in *Defects in Semiconductors 15,* Vols. 38–41 of *Materials Science Forum,* edited by G. Ferenczi (Trans Tech, Aedermannsdorf, Switz., 1989), p. 451.
[15] J. W. Corbett, *Electron Radiation Damage in Semiconductors and Metals,* Suppl. 7 of *Solid State Physics,* edited by H. Ehrenreich, F. Seitz, and D. Turnbull (Academic, New York, 1966), p. 59.
[16] S. Dannefaer, G. W. Dean, D. P. Kerr, and B. G. Hogg, Phys. Rev. B **14**, 2709 (1976).
[17] W. Fuhs, U. Holzhauer, S. Mantl, F. W. Richter, and R. Sturm, Phys. Status Solidi B **89**, 69 (1978).
[18] R. N. West, Adv. Phys. **22**, 66 (1973).
[19] B. G. Svensson and J. L. Lindström, in Ref. 3, p. 1087.
[20] J. L. Lindström, G. S. Oehrlein, and J. W. Corbett, Phys. Status Solidi A **95**, 179 (1986).
[21] S. Dannefaer, P. Mascher, and D. Kerr, J. Phys. Condens. Matter **1**, 3213 (1989).
[22] R. M. Nieminen and M. J. Manninen, in *Positrons in Solids,* edited by P. Hautojärvi (Springer-Verlag, Berlin, 1979), p. 145.
[23] W. Frank, in *Lattice Defects in Semiconductors,* IOP Conf. Proc. Ser. No. 23, edited by F. A. Huntley (IOP, London, 1975), p. 23.
[24] L. C. Kimerling, M. T. Asom, J. L. Benton, P. J. Drevinsky, and C. E. Caefer, in Ref. 14, p. 141.
[25] B. G. Svensson, K. Johnsson, D.-X. Xu, J. H. Svensson, and J. L. Lindström, Rad. Eff. Defects Solids (to be published).
[26] S. Dannefaer, P. Mascher, and D. Kerr, in Ref. 14, p. 893.
[27] B. Pagh, H. E. Hansen, B. Nielsen, G. Trumpy, and K. Petersen, Appl. Phys. A **33**, 255 (1984).
[28] M. Lax, Phys. Rev. **119**, 1502 (1960).
[29] J. Mäkinen, C. Corbel, P. Hautojärvi, P. Moser and F. Pierre, Phys. Rev. B **39**, 10 162 (1989).
[30] Y. H. Lee, J. C. Corelli, and J. W. Corbett, Phys. Lett. **60A**, 55 (1977).